



# Graphene reinforced nanocomposites: 3D simulation of damage and fracture



Gaoming Dai, Leon Mishnaevsky Jr.

Department of Wind Energy, Technical University of Denmark, Risø Campus, Frederiksborgvej 300, 4000 Roskilde, Denmark

## ARTICLE INFO

### Article history:

Received 11 May 2014

Received in revised form 7 August 2014

Accepted 8 August 2014

### Keywords:

Graphene

Nanocomposites

Damage mechanism

Crack initiation

Crack propagation

## ABSTRACT

3D computational model of graphene reinforced polymer composites is developed and applied to the analysis of damage and fracture mechanisms in the composites. The graphene/polymer interface properties are determined using the inverse modeling approach. The effect of composite structure, in particular, of the aspect ratio, shape, clustering, orientation and volume fraction of graphene platelets on the mechanical behavior and damage mechanisms of nanocomposites are studied in computational experiments. It was shown that the Young modulus of the nanocomposites increases with increasing aspect ratio, volume content, elastic properties of graphene/polymer interface layer, and decreasing the degree of intercalation. The tensile strength follows similar tendencies, except for the aspect ratio and clustering degree, where the opposite effects are observed. Nanocomposites with randomly oriented sheets of graphene demonstrate much lower Young modulus and strength as compared with the composites with the aligned graphene sheet reinforcement. It was further concluded that the structural imperfections of graphene reinforcement (like crumpling shape or random misalignment) have considerable effect on the composite performances.

© 2014 Elsevier B.V. All rights reserved.

## 1. Introduction

Graphene, a strong and light two-dimensional allotrope of carbon, attracted a growing interest of research community and industry in recent years [1–3]. Graphene sheets can be used, among others, as reinforcement in polymer composites, thus, potentially ensuring a drastic improvement of properties of the composites [4,5].

In order to explore the potential of graphene nanoreinforcements for the polymer strengthening, and to develop recommendations for the computational design of the composites, computational models linking microstructures of graphene reinforced composites with their mechanical properties and strength are necessary. A number of computational models of graphene sheets and graphene reinforced composites have been developed in recent years.

Many models are based on atomistic, combined atomistic-continuum (FE) and nanoscale-continuum approaches [1,10–12]. A detailed review of the methods of modeling of graphene and graphene based composites including Quantum Chemistry, molecular dynamics, Monte Carlo simulation and other techniques has been published by Zhang et al. [13]. Quite often, molecular dynamics (MD) simulations are employed to analyze the properties of

graphene sheets and their interaction with polymer matrix. Zhang and Gu [14] used molecular dynamics simulations to determine elastic modulus, fracture stress and fracture strain of graphene. They demonstrated that mechanical properties of graphene are much more sensitive to the temperature changes than to the layer numbers in the multilayer graphene. Li et al. [15] also used MD simulations to characterize multilayer graphene reinforced epoxy composites. They considered two configurations (graphene layers parallel and perpendicular to polymer/graphene interface), and have shown that the strengths of composites are close in both cases, while the damage mechanisms can be different: “the parallel case exhibits cohesive yield with strain localization and nano-void formation within the bulk polymer while the case with graphene sheets oriented normal to the interface exhibit interfacial debonding”. Shiu and Tsai [16] used molecular dynamics simulations, to evaluate mechanical properties of graphene reinforced nanocomposites with different morphologies (graphene platelets, intercalated graphene and intercalated graphene oxide). It was shown that the composites with intercalated graphene have a higher Young’s modulus, than do those with graphene platelets. The graphene oxide was shown to be the best reinforcement of the three considered cases. Molecular dynamics approach can deliver rather detailed information on the deformation and damage mechanisms at the nanoscale. On the other side, the continuum mechanics/finite element (FEM) based approaches can be efficiently used

E-mail addresses: [ggda@dtu.dk](mailto:ggda@dtu.dk) (G. Dai), [lemi@dtu.dk](mailto:lemi@dtu.dk) (L. Mishnaevsky Jr.)

to analyze the specimen service properties (at the macroscale). Still, it remains a challenge to link the results of the nanoscale and atomistic simulations to the continuum mechanics and strength models of the composites at the macrolevel, and to their service properties. A number of researchers directed their activities toward the development of coupled MD-continuum mechanical models or multiscale mechanical models of graphene composites. For instance, Montazeri and Rafii-Tabar [11] employed a combined method, based on the molecular dynamics, molecular structural mechanics and FEM, and determined the elastic constants of nanocomposites. Chandra et al. [17] used a multiscale FEM modeling approach to analyze the mechanical behavior of nanocomposites, and evaluate the effect of the orientation of graphene sheets on the stiffness of the composite.

While the combination of atomistic and continuum approaches could be considered as the most powerful computational tool to address the problems associated with different scales [18], these models require especially high computational costs. Further, the interface properties (which have apparently decisive effect on the properties of graphene reinforced polymers) are not always considered in these models. In order to overcome these limitations, it is suggested here to analyze the nanomaterials using “effective phases” (here, “effective interface layer” of polymer with modified properties, surrounding nanoreinforcements), the properties of which are determined using inverse modelling.

Here, we seek to develop purely continuum mechanical models of graphene reinforced nanocomposites, and employ these models to analyze microstructure–strength relationships of the materials. The objective is to explore factors controlling the strength and damage in graphene reinforced nanocomposites using the methods of micromechanics. In particular, we pay attention to the graphene/polymer interface effects, as well as the role of structural defects (weak interfaces, clustering, various orientations, etc.) on the damage initiation and fracture of the composites. In order to take into account the interface effects, we employ so-called “effective interface models” [25,26], in which the thin layers surrounding the nanoreinforcements are assumed to be from a “third”

material, with specific properties, and these properties are determined using the inverse modeling approach. The effects of nanocomposite structure, in particular, effects of the graphene platelet aspect ratio, shape, clustering, orientation and volume fraction, on the mechanical behavior and damage mechanisms of graphene nanocomposite are studied in computational experiments.

## 2. Computational model and materials properties

### 2.1. 3D finite element model of graphene monolayer composite

In order to carry our systematic computational studies of the microstructure–strength relationships of graphene reinforced polymers, a number of 3D computational models reflecting the nanocomposite structures should be generated. For this, we employ a special Python based software code developed in [19–23], and adapt it to the typical structures of graphene based composites (i.e., very high aspect ratio; thin layers). Using the code, a number of 3D FE models of graphene reinforced composites (see examples in Fig. 1) were automatically generated. The graphene sheets morphology (orientation, clustering –exfoliated or intercalated, aspect ratio) were taken into account during the model generation process. The reinforcing graphene sheets were randomly distributed in the polymer matrix and (in some models) randomly oriented. To take into account the interface effect, the generalized effective interface layer concept was used [24–26] (see more details below).

### 2.2. Implementation of damage analysis of graphene reinforced composites

The procedure of numerical simulation of damage evolution in nanocomposites includes two steps: damage onset and damage propagation [19,31].

The initial defects are introduced by subjecting the unit cell to a quasi-static load. The onset of a crack in a graphene reinforced composite is governed by the maximum principal stress criterion, which can be defined as  $f = \{\langle \sigma_{\max} \rangle / \sigma_{\max}^0\}$  [32]. Here,  $f$  denotes the

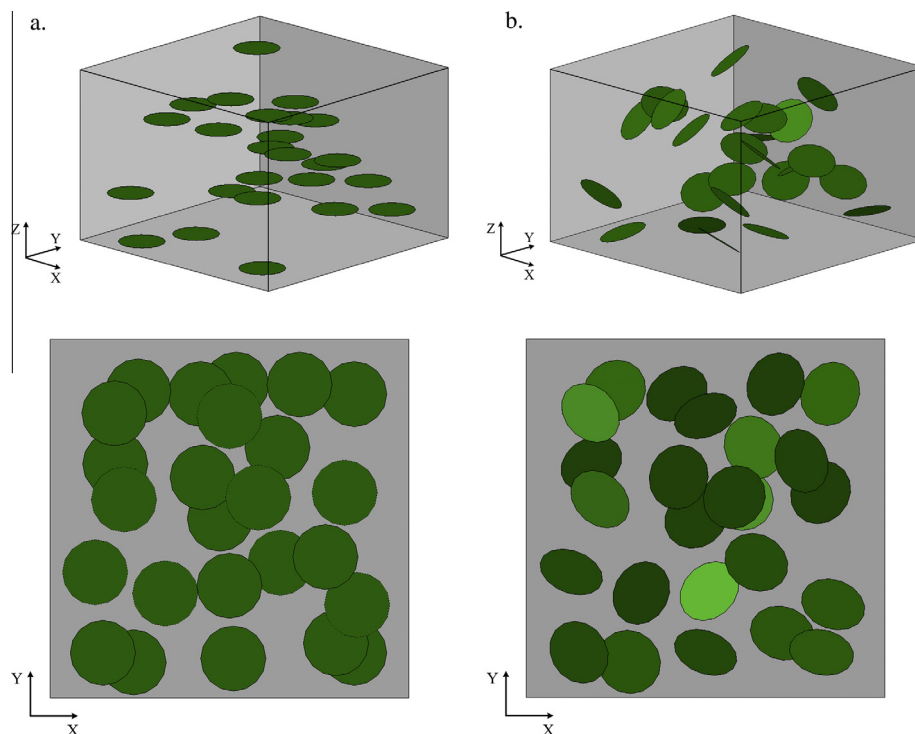


Fig. 1. Examples of 3D unit cell models of graphene reinforced composites (a). Aligned exfoliated model (b). Random exfoliated model.

maximum principal stress ratio and the initial microcrack will be formed when  $f = 1$ .  $\sigma_{\max}^0$  stands for the maximum allowable principle stress and the symbol  $\langle \rangle$  is Macaulay brackets which lets the  $\sigma_{\max}$  has the alternative value of 0 or  $m_{ix}$  when  $m_{ix} < 0$  or  $\sigma_{\max} \geq 0$ , respectively.

To model the crack propagation in graphene reinforced composites, 3D power law model is used here [33]. The power law can be described as  $(G_I/G_{Ic})^\alpha + (G_{II}/G_{IIc})^\beta + (G_{III}/G_{IIIc})^\gamma \geq 1$ . The symbol  $G_{\square}$  denotes the strain energy release rate parameters and indices  $I, II, III$  stand for the three fracture modes. The index  $c$  represents the critical values of strain energy release rate (the fracture toughness).  $\alpha, \beta, \gamma$  are parameters and are assigned the value of 1.

The numerical simulations have been carried out with the use of the commercial FE code ABAQUS/STANDARD (version 6.11). Different 3D models of graphene reinforced composites were subject to uniaxial tensile loading (displacement)  $u$  along the Z-axis direction. The three-dimensional 4-node linear tetrahedron element C3D4 is used for meshing. The virtual crack closure technique (VCCT) [34,35] is used to calculate the strain energy release rate, and the linear elastic fracture mechanics (LEFM) approach and the extended-FEM (xFEM) method [36–39] are employed to carry out the crack evolution analysis. The comparison of xFEM, cohesive zone approach and the damageable layers model as applied for the fracture modelling in composites has been presented in [31,40]. The authors demonstrated that these approaches give very similar results. With view of the efficiency of XFEM, this method has been used in the current simulations.

### 2.3. Material properties

On the basis of an analysis of literature data, the following mechanical and strength properties of graphene and matrix have been identified:

Graphene and graphene/polymer interface: thickness of the graphene sheet 0.335 nm; aspect ratios of  $3.5 \dots 7 \times 10^4$  [5]; typical diameter of 10–40  $\mu\text{m}$  [41]; Young's modulus and shear modulus of 1050 GPa [5–7] and 311 GPa [50]; tensile strength of 130 GPa [7]. maximum shear stress of 2.3 MPa at the edge of the sheet; graphene-matrix interfacial shear stress is on the order of 0.25–0.8 MPa and with a maximum value of 1 MPa [41]; fracture stress of a graphene sheet is larger than 100 GPa and the failure strain is of the order of 20% [28].

Epoxy matrix: Young's modulus of 2.13 GPa [47]; shear modulus of 1 GPa [41]; tensile strength of 49.9 MPa [47]; threshold/critical strain energy release rate of matrix [19,23], namely,  $G_{Ith} = 0.06 \text{ kJ/m}^2$ ,  $G_{Ic} = 0.173 \text{ kJ/m}^2$ ,  $G_{IIth} = 0.24 \text{ kJ/m}^2$ ,  $G_{IIc} = 0.648 \text{ kJ/m}^2$ ,  $G_{IIIth} = 0.306 \text{ kJ/m}^2$ ,  $G_{IIIc} = 0.850 \text{ kJ/m}^2$  for mode  $I, II$  and  $III$ , respectively.

### 3. Properties of graphene/polymer interface: Inverse modeling

The graphene/polymer matrix interfaces have a significant influence on the mechanical properties and strength of nanocomposites [3,28].

In this section, mechanical properties of the graphene sheets/polymer matrix interfaces are investigated using the inverse modeling. As noted in [26], the extraordinary effect of nanoreinforcement on the mechanical properties of nanocomposites (i.e., when an addition of a tiny fraction of nanoreinforcement leads to a drastic increase of elastic or strength properties, far beyond the expected “rule of mixture” estimations applicable for microscale reinforcements) is related with the interaction between the nanoreinforcements (with very high surface area) and polymer matrix, leading to the formation of a polymer layer with modified, perturbed chain structure. This layer of perturbed polymer

surrounding the nanosheets is one of the main sources of the extraordinary material strengthening, and will be modeled here using the “effective interface layer” approach [25,26].

In [24,29], the computational model of nanocomposite was developed, which includes (apart from usual matrix and reinforcement phases) a third phase, corresponding to the polymer volume surrounding the nanoreinforcements (here, graphene flakes). This “third phase” demonstrate different properties than the rest of the matrix, due to the perturbed polymer chain structures near the nanoparticles. This third phase is presented as “interphase layer” [24–26].

Here, we seek to estimate the properties of the “effective interface” around the graphene sheet, employing the inverse modeling approach [27]. Novoselov, Young and their colleagues at the University Manchester [28,41,42] studied the change in the strain distribution on a multilayer model (graphene/epoxy) and observed that the strain across the flake is uniform at the applied strain up to 0.6%. After that cracks form in polymer coating layers, with the graphene remaining intact. As a result, the interfacial shear stress in the fragments is reduced to about 0.25 MPa. Here, the cases experimentally studied in [28] are simulated numerically. The model contains three material phases: matrix, interface and graphene monolayer. The graphene monolayer has a thickness 0.34 nm, aspect ratio 2000, and is assumed to be surrounded by effective interface with a thickness of 1 nm (estimated as one half of the minimum separation between monolayer sheets given as 2 nm, see [5]). The model dimensions are  $18.4 \mu\text{m} \times 10.4 \mu\text{m} \times 0.3634 \mu\text{m}$ .

#### 3.1. Static analysis: Determination of elastic properties of the interface layer

Here, we use the iterative method to determine the Young modulus of the effective interface layer.

First, the overall range of possible variation of the effective interface properties is estimated. Apparently, the effective interface cannot be stiffer than the graphene sheet. Since “relatively poor adhesion between the graphene and polymer layers” was observed [28] and following Wang et al. [26], (who took the Young's modulus of the interface as 1/14 of matrix stiffness,  $4.2/14 = 0.3 \text{ GPa}$ ), we take the low limit at the level of 0.15 GPa.

Finite element models shown in Fig. 2 were subject to applied strains 0.4% and 0.6% along the X-direction. The initially assumed elastic module of the effective interface was taken 3.695 GPa (close to that of epoxy).

Fig. 3 shows four strain distributions along the central line/X coordinate of the graphene sheet for different interface stiffnesses. Under the 0.4% strain loading, the strain remains at almost constant level (except for a tiny drop in the middle of the graphene sheet) through the graphene sheet but falls down to 0 at the both ends. This corresponds well to the results from [28]. Under the strain 0.6%, the strain level at the central part of graphene sheet is reduced as the stiffness of the effective interface increases. It reaches the level of 0.4% when the interface has a stiffness of 3.74 GPa. The perfect “M” shape of the strain distribution along the length of graphene sheet corresponds to the experimental results by Young et al. [28] for the Young modulus of the interface 3.74 GPa.

Thus, the Young modulus of the interface layer 3.74 GPa can be used in the following simulations.

#### 3.2. Damage analysis: inverse analysis of the strength of graphene/polymer interface

Here, we seek to estimate the strength of the effective interface layer, using the inverse modeling. Again, we start with rough

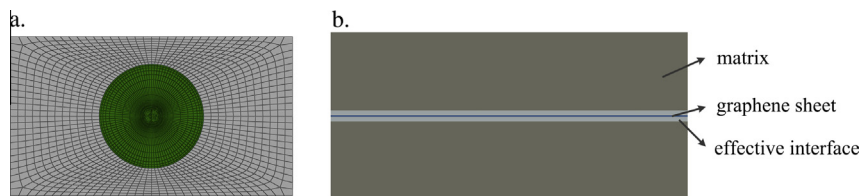


Fig. 2. A model to the inverse determination of the effective interface properties.

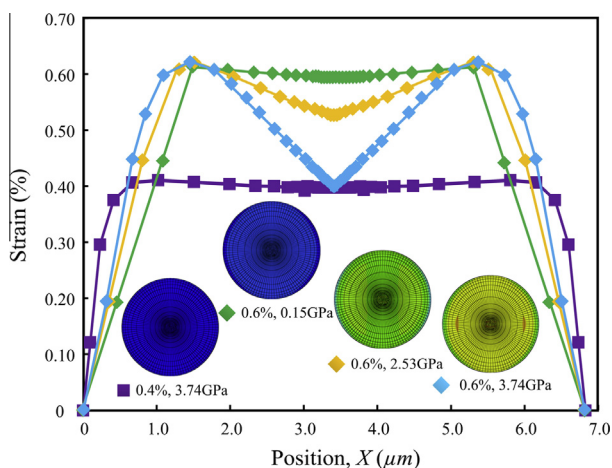


Fig. 3. Strain distribution along the X-coordinate on the central line of graphene.

estimation of the range of strength variation. In [19], the tensile strength of the nanoclay-polymer interface layer was estimated as 82 MPa. Again, taking into account the low interface strength of “graphene and polymer layers” [28], and higher aspect ratio of graphene, we take the range of the tensile strength variation of graphene sheets to be between 8.2 MPa and 82 MPa (10 times difference).

The model shown in Fig. 2 was subject to 0.8% strain loading along the X-direction (as in the experiments from [28]). The correct interface layer strength should correspond to the situation when cracks are initiated in interface when the strain loading level reaches 0.6% [28]. The Young modulus obtained in Section 3.1 has been assigned to the interface layer.

Fig. 4 gives the tensile stress–strain curves for the different interface strengths. Fig. 4a shows that the cracks are formed under strain 0.4% in the model with the interface strength 18.25 MPa. At the applied strains 0.6% and 0.8%, the material is already highly damaged. In the model with interface strength of 74.5 MPa (Fig. 4b), there is no damage even under 0.8% strain loading. In the model with the interface strength of 32.4 MPa (Fig. 4c), the material is intact under 0.4% strain. The crack is initiated under 0.6% strain loading, and the material gets quickly cracked under 0.8% strain. Thus, the strength of the effective interface can be taken (approximately) 32.4 MPa.

Further, we studied the horizontal (parallel to X-direction) shear stress distribution along the central line of a graphene sheet under different applied strains, for different interface strengths (see Fig. 5). It is found that the shear stress on the edge of graphene sheet increases (from 3.2 MPa to 4.8 MPa) as the strain loading increases (from 0.4% to 0.6%) before the interface was damaged. There is a sharp decrease of the shear stress level (from 4.8 MPa to 0.32 MPa) after the material is damaged (under 0.8% strain loading). These results correspond well to the observations by Young et al. [28].

Thus, in this section, we used the inverse modeling and the experimental data from Young et al. [28] to evaluate the elastic

and strength properties of the graphene/epoxy interface (considered as a thin layer of a polymer with modified properties). The obtained values: Young modulus 3.74 GPa and strength 32.4 MPa- will be used in our further simulations.

#### 4. Graphene morphology and crunching effect

Mechanical properties of graphene reinforced composites strongly depend on the content and distribution of graphene sheets [3]. The graphene sheets orientation (aligned and random), aspect ratio, clustering degree (intercalated and exfoliated) and volume fraction (graphene loading in the composites) have effects on the mechanical behavior of composites. In this section, we seek to analyze the effect of these parameters on the mechanical behavior of nanocomposites.

##### 4.1. Effect of graphene sheet orientation on the deformation and strength of nanocomposites

In this section, we consider the effect of graphene orientation on the mechanical properties of the composites. Several 3D unit cell models with 25 graphene sheets with aspect ratio 2000 (graphene fraction of 0.50%) and varied graphene orientations (aligned/random) were generated (Fig. 1). The graphene nanosheets in the aligned models are parallel to the X–Y plane while the graphene nanosheets in the random model are assigned random angles with the plane (in the range of 0–65°).

Fig. 6 the stress–strain curves for aligned and random arranged graphene models subject to normal and axial loadings. (Here, Z is the direction of loading, means the loading normal to the graphene sheets, and X direction means the loading along the graphene sheets).

The composites with aligned graphene sheets demonstrate a higher Young’s modulus (3.52 GPa in X direction and 3.27 GPa in Z direction versus 1.915 GPa in X direction and 1.84 GPa in the Z direction for the material with random orientations) and higher ultimate strength (106.76 MPa and 89.56 MPa in X and Z direction, respectively, when versus 40.91 MPa and 38.82 MPa for the random models). Thus, the misalignment of nanosheets leads to the reduction of Young’s modulus of the composites by 43.76%, and to the 56.65% decrease of strength (with the Z direction loading).

The stress–strain curve of the model with random reinforcement is more zigzagged than that with aligned reinforcement. This can be interpreted in the sense that the misalignment of graphene sheets can delay the crack propagation.

Fig. 7 shows the cracks morphology in the unit cells with aligned and random graphene sheets distributions, respectively. One can see that a crack initiates at the graphene–matrix interfaces in both cases. Then it grows throughout the whole interface region and propagates into the matrix. Cracks meet in the matrix and merge together to form the main crack. One can observe that the main damage/toughening mechanisms in the case of a composite with aligned sheets are debonding and crack deflection.

Further damage mechanisms such as crack pinning and crack bridging are observed in the material with randomly oriented sheets.

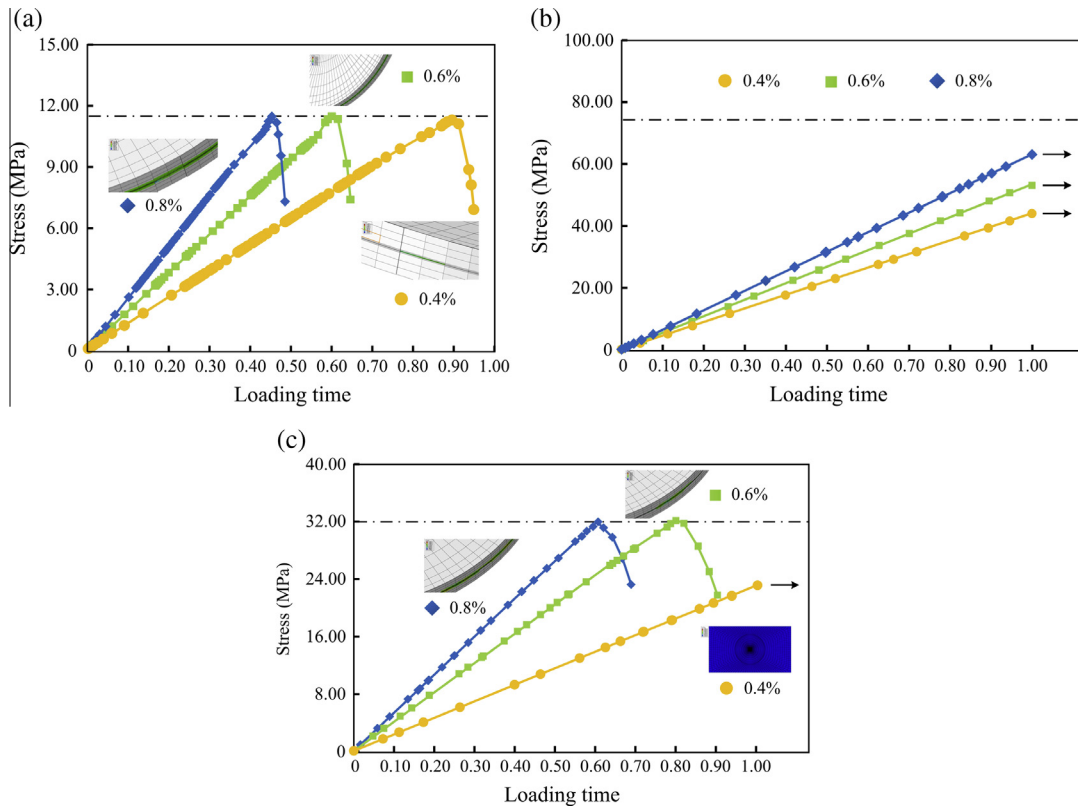


Fig. 4. Stress–loading time relationship under different strain loading and different interface strength as (a) 18.2 MPa, (b) 74.5 MPa, (c) 32.4 MPa.

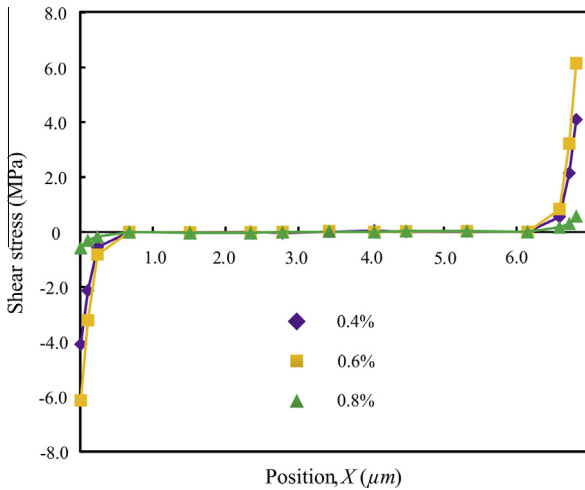


Fig. 5. Shear stress level along the X direction.

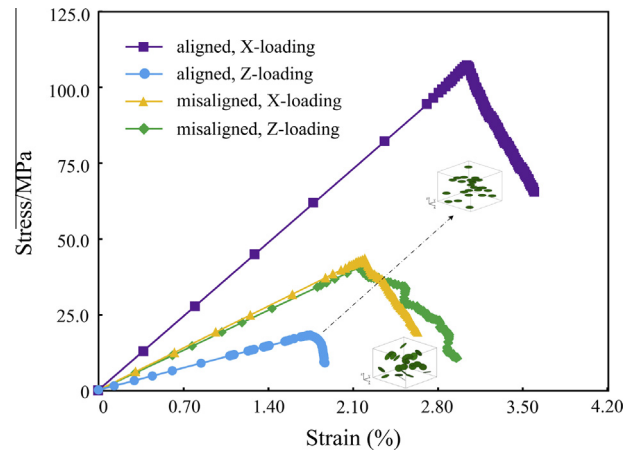


Fig. 6. Strain–stress relationship composites with aligned and random graphene reinforcement.

4.2. Effect of aspect ratio of graphene on the deformation and strength of nanocomposites

Here, we consider the effect of aspect ratio of graphene sheets on the mechanical behavior of graphene reinforced polymer composites.

Several 3D unit cells with varied aspect ratios of graphene sheets were generated. The volume content of graphene was 0.5% (25 graphene sheets per unit cell). The aspect ratios of graphene sheets were taken 1000, 2000, 10,000 and 20,000.

Fig. 8 shows the stress–strain curves for the considered cases. One can see that the material with the aspect ratio of graphene 1000 shows the highest tensile strength (114.71 MPa) and lowest Young’s modulus (2.91 GPa), while the nanocomposite with aspect

ratio sheets 20,000 show the lowest tensile strength (46.94 MPa, 59% lower) but the highest Young’s modulus (3.667 GPa, 26% higher). Similar results have been reported by Boo et al. [43].

It is known that for the fibrous reinforcement, there exist a critical aspect ratio after which the positive effect of enlargement of fiber length becomes weak or even negligible. In different works, the critical aspect ratios for carbon nanotubes have been estimated at the level of 200–300 [44,45]. As shown by Mortazavi et al. [46], the critical aspect ratio increases when the contrast in properties of the matrix and reinforcement increases. In our simulations, the considered aspect ratios are significantly higher than the values estimated in these and other works. That explains relatively weak influence of the aspect ratios of graphene reinforcements observed in the simulations.

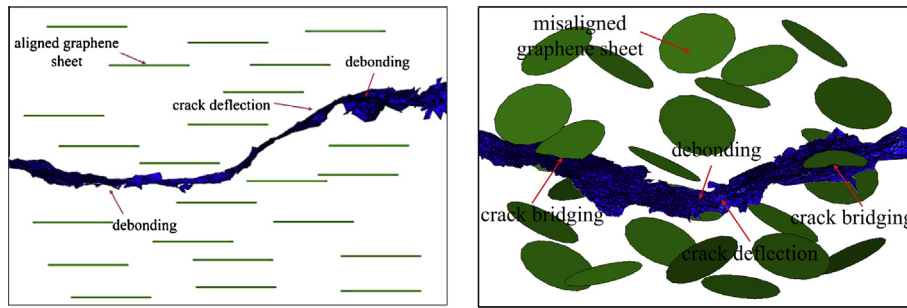


Fig. 7. Crack morphology in an aligned and random model.

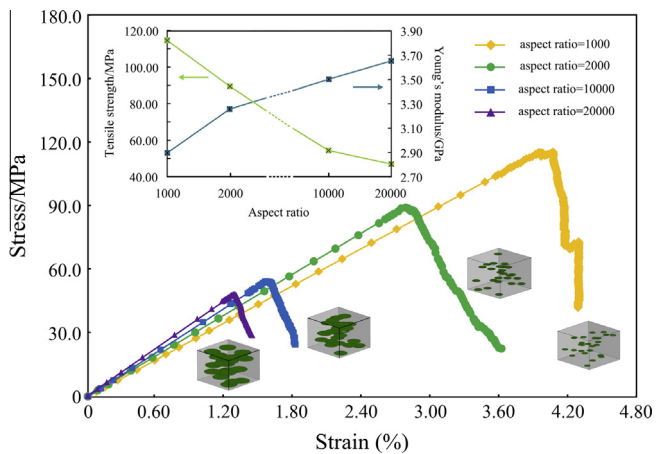


Fig. 8. Graphene reinforced composites: aspect ratio effects.

#### 4.3. Effect of graphene clustering

Currently, the goal to fabricate truly exfoliated graphene composite is still far from being achieved [3]. Graphene sheets in the composites are quite often stacked or intercalated [4].

In this section, the effect of clustering of graphene sheets on the mechanical properties of nanocomposites is studied.

Several 3D unit cell models with 25 exfoliated graphene sheets and with 5 clusters (each cluster with 5 graphene sheets) as well as with 3 graphene monolayers plus 4 clusters with clustering degree of 2 (2 graphene sheets in one cluster), 3 clusters with clustering degree of 3 and one 5 degree cluster were generated and tested in the simulations. The volume content of graphene was 0.5%.

As differed from the modeling concept of nanocomposites used by Dai and Mishnaevsky [22] earlier, the effective interfaces in the current models were built only around graphene sheets or cluster (i.e., between graphene sheets or graphene clusters, and the matrix), but not between graphene sheets inside the clusters. This modification was motivated by the experimental observations by Gong et al. [8], who estimated the thickness of graphene trilayer as 1 nm (just 3 times of the monolayer thickness, 0.34 nm) and Mahmoud [30] (who measured the thickness of four layers graphene sheets as 1.4 nm, 4 times of a single graphene sheet). It also means that the internal debonding between graphene in each graphene multilayer cluster was neglected.

Fig. 9 shows the stress–strain curves for the unit cells with different degrees of clustering.

One can see that the tensile strength increases as the clustering degree of nanoreinforcement increases (from 89.56 MPa for the exfoliated structure model to 108.55 MPa for the model with cluster degree of 5, what gives an increase of 21.2%). The Young's modulus of nanocomposite decreases with the increasing clustering (from 3.270 GPa to 2.454 GPa, with the decrease of 25%). When

the graphene sheets are clustered, their effective aspect ratio decreases. On the other side, mechanical properties of the clusters become transversely isotropic and not homogenous. This has a strong influence on the mechanical properties of composites.

#### 4.4. Volume content effects

Now, we seek to analyze the effect of the volume fraction of graphene on the mechanical properties and strength of graphene reinforced composites. A number of unit cell models with different graphene contents (0.25%, 0.50% and 1.00%) were generated and tested.

Fig. 10a shows that the volume fraction of graphene in the nanocomposites has a significant effect on the mechanical behavior and damage resistance of the nanocomposites. The unit cell model with graphene content 1.00% has the highest tensile strength (111.67 MPa) and Young's modulus (5.9 GPa) while the model with 0.25% graphene content has the lowest tensile strength and Young's modulus of 75.16 MPa and 2.41 GPa, respectively. It is apparent that the mechanical performances of the composites exhibit a dramatic improvement due to the graphene reinforcement.

Comparing the graphene reinforced nanocomposite (0.50% graphene) with pure polymer, one can see that the tensile strength and the Young's modulus are 79.44% higher (from 49.9 MPa to 89.56 MPa) and 53.52% higher (from 2.13 GPa to 3.27 GPa) in the nanocomposite, respectively. Thus, the effect of graphene nanoreinforcements is far stronger than the “rule of mixture” estimation.

It can be concluded that the graphene reinforcement has a very strong influence on the mechanical properties of composites. The tensile strength and Young's modulus of the composites both increased as the volume fraction of graphene sheets increased.

### 5. Graphene shape and interfacial properties effect

According to Singh et al. [3], “controlling the folding, crumpling and bending of graphene materials” and “understanding of the interfacial structure and properties” are two of the five main challenges in producing idle graphene reinforced composites.

In this section, the effects of graphene sheet crumbling and the interfacial properties on the nanocomposite performances are studied numerically.

#### 5.1. Effect of crumpled graphene on the deformation and strength of nanocomposites

The shapes of graphene sheets in polymers are usually far from ideal discs. The graphene sheets have rather often bent, crumpled and waived shapes [4]. When dispersed in the polymer matrix, graphene sheets can adopt wavy or wrinkled forms, which may also reduce the moduli.

In this section, we study the effect of crumpled graphene sheet on the mechanical properties of graphene reinforced composites.

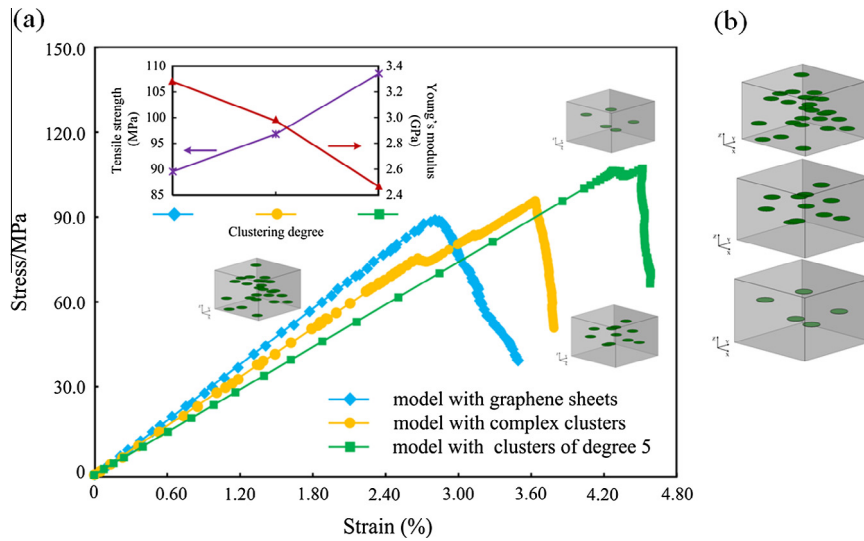


Fig. 9. Clustering effect upon the mechanical behavior of graphene reinforced composites (a) and models with different clustering degrees (b).

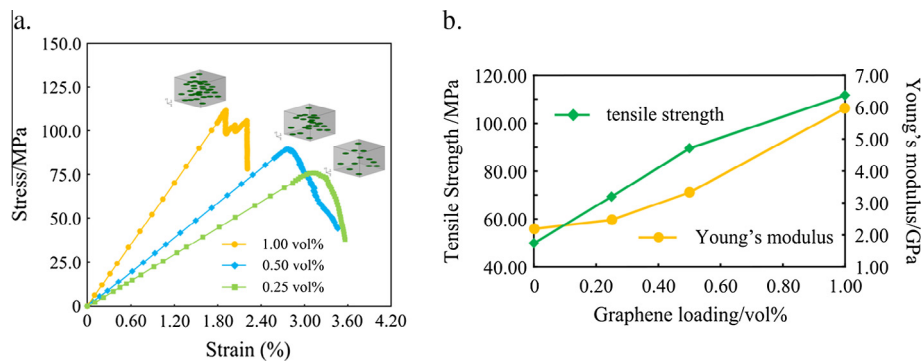


Fig. 10. Volume fraction effects on the mechanical behavior of graphene reinforced nanocomposites (a) stress–strain curves and (b) tensile strength and Young's modulus versus graphene loading.

The polygon graphene sheet (which Gong et al. [41] considered in their work) is modeled here (Fig. 11b–d). The polygon graphene sheet has a dimension of  $12\ \mu\text{m}$  and  $34\ \mu\text{m}$  in  $X$  and  $Y$  directions, respectively. The whole model has a dimension of  $24\ \mu\text{m} \times 45\ \mu\text{m} \times 15\ \mu\text{m}$  along the  $X$ ,  $Y$  and  $Z$  directions. Also, a crumpled version of the polygon graphene sheet model was generated on the basis of the polygon model (Fig. 11c).

Fig. 11a shows the stress–strain curves, estimated elastic and strength properties for these two cases. As expected, the flat graphene model is strongly preferable over the crumpled graphene. The flat graphene model shows tensile strength of 83.53 MPa while the crumpled one corresponds to 38.83 MPa, (53.52% decrease). Also, Young modulus is 9.49% lower for the model with crumpled graphene (from 2.107 GPa to 1.907 GPa).

One can see that the strength of composites is much more sensitive to the shape imperfections of graphene sheets than their elastic properties.

One should be also noted that graphene is in fact a highly flexible material while in our models it is represented as a rigid body (due to its high elastic modulae). While it is beyond the current study, this aspect of graphene deformation will be incorporated in our following simulations. This issue is especially important for crumpled graphene.

## 5.2. Interfacial strength and its effect on the material behavior

In several works, the potential of chemical functionalization of graphene for improving the interfacial bonding between graphene

and polymers, and ultimately, its reinforcing properties, were studied [4,48,49].

Here, we consider the effect of the interface layer strength on the mechanical properties and strength of the composite.

A number of 3D unit cell models with 25 aligned graphene sheets (aspect ratio 2000, and volume content 0.5%) were generated. Different interfacial strengths were assigned to the interface layers (67, 198 and 514 MPa).

Fig. 12 shows the results of simulations. One can see that the material with strong interfaces (514 MPa) ensures the highest tensile strength (127.94 MPa), Young's modulus (3.687 GPa) and largest elongation till failure. The material with weakest interface (67 MPa) has the lowest tensile strength (50.29 MPa), Young's modulus (2.873 GPa) and elongation. Thus, the strong interface is indeed an important resource for the improvement of the mechanical properties of graphene reinforced composites. Young et al. [28] also noticed that forming strong interfaces between matrix and graphene can provide nanocomposites with “reasonable stiffness, and strength”.

## 6. Discussion

It is of interest to compare the results of numerical experiments with some literature data. Using the inverse analysis, we determined the elastic modulus of the polymer layer surrounding the graphene sheets, which is  $3.74/2.14 = 75\%$  higher than the elastic modulus of polymer matrix. This corresponds to the results by Shiu

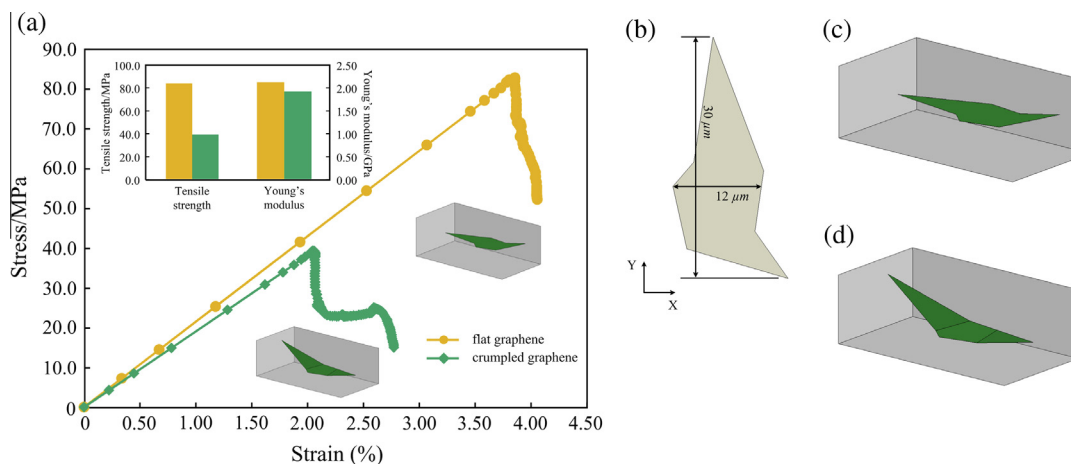


Fig. 11. Crumpled effects upon the graphene reinforced composites (a), and schema of crumpled (d) and plain (c) sheets and their dimensions (b).

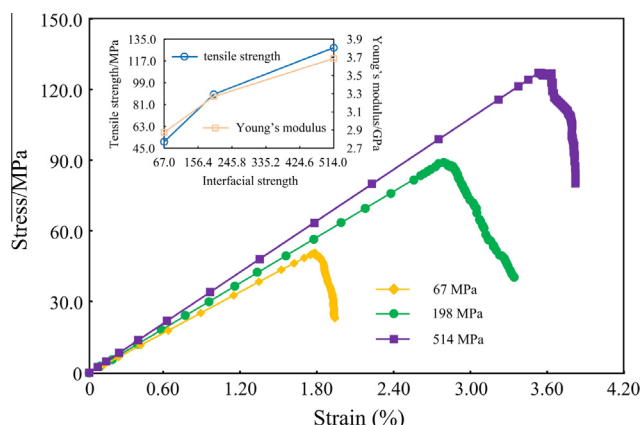


Fig. 12. Interfacial properties effects on the material behavior.

and Tsai [16], who observed the morphology of polymer chains near the graphene sheets and found that “the local density close to the graphene is relatively high, and there are greater amounts of high density polymers in the intercalated graphene nanocomposites. These high amounts of high density polymer are responsible for the enhanced thermal and mechanical properties in the intercalated nanocomposites”.

In Section 4.4, we observed that if comparing the graphene reinforced nanocomposite (0.50% graphene) with pure polymer, the tensile strength and Young's modulus are 79.44% and 53.52% higher, respectively. According to Liang et al. [47], the tensile strength and Young's modulus increase by 76% and 62%, respectively when 0.41 vol.% of graphene sheets are introduced into PVA matrix. Zhao et al. [49] showed that the tensile strength of graphene sheets reinforced composite with 0.6% graphene is 73% higher than that of pure matrix, while the Young's increases by 150% (however, the aspect ratio of graphene sheets in their materials is larger and is up to 3000–6000). These evaluations are in fact very close to our computational estimations of the effect of graphene reinforcement on the polymer properties (79%, 53%).

In Section 4.1, we studied the cracks morphology in the composites with aligned and randomly oriented sheets. It was observed that a crack initiates at the graphene–matrix interface in both cases. This corresponds to the observation by Gong et al. [8] that the adhesion between graphene and polymer is relatively poor. Then the crack grows throughout the whole interface region and propagates into the matrix, they deflect on the nanosheets. Also,

Shadlou et al. [9] observed the crack deviations on nanoparticles and crack propagation along the interfaces as most typical crack growth mechanisms in epoxy nanocomposites with various carbon nanoreinforcements.

In Section 4.3, it was demonstrated that the graphene clustering leads to the higher stiffness of the graphene reinforced composites. This is confirmed by the results of the molecular dynamics simulations by Shiu and Tsai [16] who showed that composites with intercalated graphene have a higher Young's modulus, than those with graphene platelets. The effect of the graphene aspect ratio on the composite properties, observed in Section 4.2 is relatively weak: only 26% higher stiffness as a result of the 20 times higher aspect ratio. However, this corresponds also to results by Chandra et al. [17], who observed that “... the stress–strain curves obtained do not show a considerable dependence of the results on the length of the graphene reinforcement”.

## 7. Conclusions

In this paper, microstructure–mechanical properties and – strength relationships of graphene reinforced polymer nanocomposites are investigated numerically, using 3D micromechanical unit cell models. The elastic and strength properties of the thin interface layer between graphene sheets and epoxy polymer are determined using the inverse modeling method. The effect of microstructure of graphene based composite, in particular, aspect ratio, shape (crumpled versus flat) and orientation of graphene sheets, their clustering, on the stress–strain curves, tensile strength and elastic properties of the nanocomposite are studied.

Summarizing the presented numerical experiments, one can draw the following conclusions. The Young modulus of nanocomposites increases with increasing the aspect ratio, volume content, strength of interface layer and decreases with the higher degree of graphene sheet clustering. The tensile strength follows similar tendencies, except for the aspect ratio and clustering degree, where the opposite effects are observed. Randomization of nanoplatelet orientation leads to the strong reduction of Young modulus and strength of the nanocomposite, as compared with the case of a composite with aligned graphene sheets.

The factors influencing the elastic properties and strength of nanocomposites can be ranked as follows (from stronger to weaker effects): crumpled graphene shape (only for strength: 50% reduction of strength only due to the shape crumpling, but only 10% reduced stiffness) -> graphene sheet misalignment (~50% reduction of stiffness and strength because of misalignment) -> volume content of graphene (50% higher stiffness and 2.5 times higher strength at 4 times higher content of graphene) -> interface

strength (7 times higher interface strength gives only 2.5 times higher composite strength) and clustering degree (only 25% difference between highly clustered and exfoliated) → the aspect ratio of sheets (~60% lower strength and 26% higher stiffness due to 20 times higher aspect ratio). (The ranking is conditional, still, it shows that the structural imperfections in graphene reinforced composites, like sheet crumpling and misalignment, have the strongest effect on the composite properties).

### Acknowledgements

The author gratefully acknowledges the financial support of the Danish Council for Strategic Research (DSF) via the Sino-Danish collaborative project “High reliability of large wind turbines via computational micromechanics based enhancement of materials performances” (Ref. No. 10-094539). Furthermore, the author is grateful to the DSF for its support via the Danish Centre for Composite Structures and Materials for Wind Turbines (DCCSM) (Contract No. 09-067212).

### Appendix A. Supplementary material

Supplementary data associated with this article can be found, in the online version, at <http://dx.doi.org/10.1016/j.commatsci.2014.08.011>.

### References

- [1] A.K. Geim, K.S. Novoselov, *Nat. Mater.* 6 (2007) 183–190.
- [2] A.K. Geim, *Science* 324 (2009) 1530–1534.
- [3] V. Singh, D. Joung, L. Zhai, S. Das, S.I. Khondaker, S. Seal, *Prog. Mater. Sci.* 56 (2011) 1178–1271.
- [4] J.R. Potts, D.R. Dreyer, C.W. Bielawski, R.S. Ruoff, *Polymer* 52 (2011) 5–25.
- [5] R.J. Young, I.A. Kinloch, L. Gong, K.S. Novoselov, *Compos. Sci. Technol.* 72 (2012) 1459–1476.
- [6] C. Lee, X.D. Wei, J.W. Kysar, J. Hone, *Science* 321 (2008) 385–388.
- [7] F. Liu, P.B. Ming, J. Li, *Phys. Rev. B* 76 (2007) 064120.
- [8] L. Gong, R.J. Young, I.A. Kinloch, I. Riaz, R. Jalil, K.S. Novoselov, *ACS Nano* 6 (2012) 2086–2095.
- [9] S. Shadlou, E. Alishahi, M.R. Ayatollahi, *Compos. Struct.* 95 (2013) 577–581.
- [10] Y. Chandra, F. Scarpa, R. Chowdhury, S. Adhikari, J. Sienz, *Compos. Part A: Appl. Sci. Manuf.* 46 (2013) 147–153.
- [11] A. Montazeri, H. Rafii-Tabar, *Phys. Lett. A* 375 (2011) 4034–4040.
- [12] M.M. Shokrieh, R. Rafiee, *Mater. Des.* 31 (2010) 790–795.
- [13] T. Zhang, Q. Xue, S. Zhang, M. Dong, *Nano Today* 7 (3) (2012) 180–200.
- [14] Y.Y. Zhang, Y.T. Gu, *Comput. Mater. Sci.* 71 (2013) 197–200.
- [15] F. Li, N. Yan, Y. Zhan, et al., *J. Appl. Polym. Sci.* 129 (4) (2013) 2342–2351.
- [16] S.C. Shiu, J.L. Tsai, *Compos. Part B: Eng.* 56 (2014) 691–697.
- [17] Y. Chandra, F. Scarpa, R. Chowdhury, S. Adhikari, J. Sienz, *Compos. Part A: Appl. Sci. Manuf.* 46 (2013) 147–153.
- [18] B. Mortazavi, O. Benzerara, H. Meyer, J. Bardon, S. Ahzi, *Carbon* 60 (2013) 356–365.
- [19] G.M. Dai, L. Mishnaevsky Jr., *Compos. Sci. Technol.* 91 (2014) 71–81.
- [20] L. Mishnaevsky Jr., G.M. Dai, *Comput. Mater. Sci.* 81 (2014) 630–640.
- [21] L. Mishnaevsky Jr., G. Dai, *Compos. Struct.* 117 (2014) 156–168.
- [22] G.M. Dai, L. Mishnaevsky Jr., *Compos. Sci. Technol.* 74 (2013) 67–77.
- [23] G.M. Dai, L. Mishnaevsky Jr., *Compos. Sci. Technol.* 94 (2014) 71–79.
- [24] G.M. Odegard, T.C. Clancy, T.S. Gates, *Polymer* 46 (2005) 553–562.
- [25] R.D. Peng, H.W. Zhou, H.W. Wang, L. Mishnaevsky Jr., *Comput. Mater. Sci.* 60 (2012) 19–31.
- [26] H.W. Wang, H.W. Zhou, R.D. Peng, L. Mishnaevsky Jr., *Compos. Sci. Technol.* 71 (2011) 980–988.
- [27] L. Mishnaevsky Jr., *Compos. Sci. Technol.* 72 (2012) 1167–1177.
- [28] R.J. Young, L. Gong, I.A. Kinloch, I. Riaz, R. Jalil, K.S. Novoselov, *ACS Nano* 5 (2011) 3079–3084.
- [29] L. Mishnaevsky Jr., P. Brondsted, *Mater. Sci. Eng.: A* 498 (2008) 81–86.
- [30] W.E. Mahmoud, *Eur. Polym. J.* 47 (2011) 1534–1540.
- [31] H.W. Wang, H.W. Zhou, L. Mishnaevsky Jr., P. Brondsted, L.N. Wang, *Comput. Mater. Sci.* 46 (2009) 810–820.
- [32] F. Greco, L. Leonetti, P.N. Blasi, *Eng. Fract. Mech.* 80 (2012) 92–113.
- [33] V.K. Goyal, E.R. Johnson, C.G. Davilia, *Compos. Struct.* 65 (2004) 289–305.
- [34] E.F. Rybicki, M.F. Kanninen, *Eng. Fract. Mech.* 9 (1977) 931–938.
- [35] R. Krueger, *Appl. Mech. Rev.* 57 (2004) 109–143.
- [36] T. Belytschko, R. Gracie, G. Ventura, *Modell. Simul. Mater. Sci. Eng.* 17 (2009) 1–24.
- [37] T. Belytschko, T. Black, *Int. J. Numer. Meth. Eng.* 45 (1999) 601–620.
- [38] M. Stolarska, D.L. Chopp, N. Moes, T. Belytschko, *Int. J. Numer. Meth. Eng.* 51 (2001) 943–960.
- [39] N. Sukumar, N. Moes, B. Moran, T. Belytschko, *Int. J. Numer. Meth. Eng.* 48 (2000) 1549–1570.
- [40] H.W. Wang, H.W. Zhou, H.W. Ji, X.C. Zhang, *Mater. Des.* 55 (2014) 191–196.
- [41] L. Gong, I.A. Kinloch, R.J. Young, I. Riaz, R. Jalil, K.S. Novoselov, *Adv. Mater.* 22 (2010) 2694–2697.
- [42] L. Gong, R.J. Young, I.A. Kinloch, I. Riaz, R. Jalil, K.S. Novoselov, *ACS Nano* 6 (2012) 2086–2095.
- [43] W.J. Boo, L. Sun, G.L. Warren, E. Moghbelli, H. Pham, A. Clearfield, et al., *Polymer* 48 (2007) 1075–1082.
- [44] A. Needleman et al., *Compos. Sci. Technol.* 70 (15) (2010) 2207–2215.
- [45] J.N. Coleman et al., *Carbon* 44 (9) (2006) 1624–1652.
- [46] B. Mortazavi, J. Bardon, S. Ahzi, *Comput. Mater. Sci.* 69 (March 2013) 100–106.
- [47] J.J. Liang, Y. Huang, L. Zhang, Y. Wang, Y.F. Ma, T.Y. Guo, Y.S. Chen, *Adv. Funct. Mater.* 19 (2009) 1–6.
- [48] C. Lv, Q.Z. Xue, D. Xia, M. Ma, *Appl. Surf. Sci.* 258 (2012) 2077–2082.
- [49] X. Zhao, Q.H. Zhang, D.J. Chen, *Macromolecules* 43 (2010) 2357–2363.
- [50] J.L. Tsai, S.H. Tzeng, Y.T. Tzou, *Int. J. Solids Struct.* 47 (2010) 503–509.